



RESEARCH PAPER

A Smartphone-integrated Approach to Blood Pressure Estimation: Combining Video PPG and Pre-trained Convolutional Neural Networks

Gustavo dos Santos Menezes Alves  [Universidade Estadual de Feira de Santana | gustavoeu2017@gmail.com]

Cláudio Eduardo Góes   [Universidade Estadual de Santa Cruz | cegoes@uesc.br]

 Department of Exact Sciences, Universidade Estadual de Santa Cruz, Campus Soane Nazaré de Andrade, Rod. Jorge Amado, Km 16 - Salobrinho, Ilhéus, BA, 45662-900, Brazil.

Abstract. Non-invasive blood pressure estimation using photoplethysmography signals and artificial neural networks represents a promising advancement in cardiovascular health monitoring. The global prevalence of cardiovascular diseases and the demand for more accessible and practical cardiac health monitoring solutions drive this innovative approach. By leveraging smartphone camera technology to capture photoplethysmography signals, which are subsequently processed by neural network-based software, this method demonstrates significant potential. Results showed notable performance in estimating systolic blood pressure, achieving a mean absolute error of 5.65 ± 3.27 mmHg. Compared to related studies, the proposed method exhibited a lower error rate, surpassed only by a specific study by Yuriy Kurylyak, which reported a mean absolute error of 3.80 ± 3.46 mmHg for SBP estimation. However, the prediction of diastolic blood pressure showed a slightly higher error, with a mean absolute error of 7.51 ± 4.65 mmHg. The significance of this research lies in introducing a promising non-invasive approach to blood pressure estimation, potentially facilitating early detection and more efficient monitoring of cardiac conditions. Furthermore, the implementation of a blood pressure classification system and the potential expansion to mobile devices enhance user convenience and flexibility.

Keywords: Photoplethysmography, Blood Pressure, Cardiovascular Monitoring, PPG Signal, Computer Vision, Deep Learning

Received: 13 March 2025 • Accepted: 26 May 2025 • Published: 08 June 2025

1 Introduction

According to data from the World Health Organization (WHO), the number of adults with hypertension between 30 and 79 years old increased from 650 million to 1.28 billion during the period 1990-2019. Hypertension significantly influences the risk of heart, kidney, and brain diseases, among others. It's one of the leading causes of death and disease worldwide. This condition can be clearly identified through blood pressure measurement and can, in most cases, be effectively treated with controlled, low-cost medications [Zhou *et al.*, 2021].

In Brazil, hypertension is responsible for approximately 40% of heart attacks, 80% of strokes, and 25% of cases of end-stage renal failure. About 25% of the adult population in Brazil suffers from hypertension, and in people over 60 years old, this number reaches 50% [Moreira, 2018]. Hypertension can be asymptomatic in patients, a characteristic that justifies its designation as a silent disease. However, despite this disease not demonstrating some symptoms, it can bring serious consequences to the patient. According to Moreira [2018], the most efficient way to monitor blood pressure is through consistent monitoring. With this behavior it is possible to determine which treatment should be prescribed.

As reported by Ibtehaz and Rahman [2020b], the widely used method for measuring blood pressure is based on cuffs. However, it is important to emphasize that these methods can cause certain inconvenience to patients. In these authors' study, it is further highlighted that this method is not particularly suitable for continuous blood pressure monitoring. As

a result, there has recently been growing interest within the research community in developing methods and devices to determine blood pressure from biomedical signals in a continuous and non-intrusive manner.

Photoplethysmography (PPG) has gained significant popularity in recent times due to its widespread inclusion in technologies such as smartwatches, owing to its simplicity and low cost [Ibtehaz and Rahman, 2020b]. PPG measures changes in blood volume by means of light incidence on the skin, calculating its alterations as a function of light absorption. The signal obtained from PPG is associated with changes in arterial blood volume, as the pulsatile component of blood volume is primarily caused by arterial pressure pulsation over the cardiac cycle [Leal, 2019].

This study aims to determine blood pressure using alternative methods to traditional approaches and is divided into four parts: acquisition of cardiac pulse signals captured through videos of the index finger, processing of this signal using photoplethysmography, utilization of a neural network employed in the system to estimate blood pressure, and finally, a statistical analysis between the pressures estimated by the system and the results found using a digital measurement device.

2 Fundamentation

The following subsections present a brief description of the fundamental concepts for the development of this work.

2.1 Arterial System

The main function of the arterial system is the distribution of blood to capillary beds throughout the body. Arterioles are the high-resistance vessels of this system, regulating flow distribution to various capillary beds. Blood flows through conduits of considerable volume and distensibility, ranging from the (elastic) aorta to high-resistance terminations, forming a hydraulic filter similar to that of electrical systems (resistance-capacitance), converting the intermittent flow from the heart into continuous flow through the capillaries [Berne *et al.*, 2008]. This process reduces the heart's workload.

2.1.1 Blood Pressure

Blood pressure (BP) is a measure of the force that blood exerts on arterial walls. It consists of two main values: systolic blood pressure (SBP) and diastolic blood pressure (DBP) [Junqueira, 2006]. During the heart's contraction phase, known as ventricular systole, blood is ejected into the arteries, resulting in blood accumulation and increased arterial pressure. This maximum value reached is called SBP. As blood is distributed to body tissues and the ventricles enter the relaxation phase, called diastole, arterial pressure gradually decreases until it reaches its minimum value, known as DBP. Normal BP values for SBP are up to 140 mmHg, while normal DBP are up to 90 mmHg. On average, normal blood pressure values are around 120 mmHg for systolic and 80 mmHg for diastolic.

BP is determined by cardiac output multiplied by peripheral resistance as shown in equations 1 and 2 below.

Cardiac Output (CO):

$$CO = HR \times SV \quad (1)$$

where:

- HR = Heart Rate (number of heartbeats per minute);
- SV = Stroke Volume (volume of blood ejected with each heartbeat).

Blood Pressure (BP):

$$BP = CO \times PR \quad (2)$$

where:

- PR = measure of resistance that blood vessels offer to blood flow.

2.1.2 Changes in Blood Pressure

It is important to emphasize that without BP, blood would not flow through vessels, given that this movement occurs due to pressure differences between points in the vessels. The problem exists when BP is unstable or outside normal ranges, whether in hypotension or hypertension. Various factors can influence BP changes, causing either increases or decreases. Some of these factors may be associated with an intrinsic dysfunction in the circulatory system, or even with a stress event experienced by the individual [Moreira, 2018].

The condition of hypotension can be caused by hemorrhage, for example, considering here an internal hemorrhage caused by vessel rupture, cardiac pump failure, and

vasodilation. In the case of hypertension, besides external factors such as stress, some of the internal factors that cause increased pressure are water and sodium retention, vasoconstriction, increased blood demand, increased blood viscosity, and arterial stiffening [Moreira, 2018].

2.1.3 Conventional Blood Pressure Monitoring Methods

There is a clinical guideline that encourages sporadic blood pressure monitoring in the home environment, when feasible, given that evaluation exclusively in the healthcare center does not provide an accurate and reliable representation.

It is stated that routine monitoring in the medical office is essential for checking BP, but it is still highly recommended that people perform daily monitoring to track treatment, improve adherence, and control BP [Sousa *et al.*, 2011].

2.1.4 Methods and Instruments for Blood Pressure Monitoring

In 1856, the first more accurate blood pressure measurement in a human was performed during surgery by Faivre [Introcaso, 1998]. A pressure of 120 mmHg was detected in the femoral artery, while in the brachial artery these values varied between 115 and 120 mmHg, initiating the search for stability values. In 1896, Scipione Riva-Rocci created a more portable sphygmomanometer, which consisted of a cuff that covered the arm around its entire circumference, which was inflated until the radial pulse completely disappeared and then deflated until its reappearance, thus measuring blood pressure [Kohlmann and Kohlmann Jr, 2011].

Some modifications were made to this sphygmomanometer and other developments that led to the emergence of auscultatory. The most common method used in medical offices is auscultatory. This type of instrument uses the technique that determines blood pressure by monitoring Korotkoff sounds. This technique is performed using a manometer coupled to an inflatable bag (cuff), as shown in Figure 1, and a stethoscope.

This method aims to interrupt blood flow in the brachial artery by inflating the cuff and then slowly releasing the air from the bag and, using the stethoscope, perceiving the noise produced when flow returns. When blood begins to flow through the artery, its flow creates a synchronous pulse (first



Figure 1. Auscultatory method. Source: Suárez [2003]



Figure 2. Digital and automatic blood pressure measuring device. Oscillometric method. Adapted from: Hsu *et al.* [2020]

Korotkoff sound) [Moreira, 2018].

With advances in technology, it was possible to develop new techniques involving digital signal processing to measure blood pressure, such as oscillometry and PPG. The oscillometry technique (Figure 2) also uses the same idea of occluding flow to determine BP. The equipment pressurizes the cuff to detect oscillometric pulses. To determine BP, this technique identifies, quantifies, and analyzes these pulses at the points where oscillations are greatest [Moreira, 2018].

2.2 Photoplethysmography

Light radiation permeates biological tissue and can be absorbed by various substances, including skin pigments, bone structures, and components of arterial and venous blood. Arteries contain more blood volume during the systolic phase of the cardiac cycle than during the diastolic phase [Galloway, 2012]. PPG sensors optically detect changes in blood flow volume in the microvascular bed of tissue through reflection or transmission, as shown in Figure 3.

The passage of light through human tissue can be absorbed by skin, bones, and arterial and venous blood, as shown in Figure 4. The optical receiver detects changes in reflected light intensity due to changes in blood flow volume. The incident light is amplitude-modulated by changes in blood volume during the cardiac cycle, with maximum blood volume occurring in the systolic phase and minimum blood volume in the diastolic phase [Kalkhaire and Puranik, 2016].

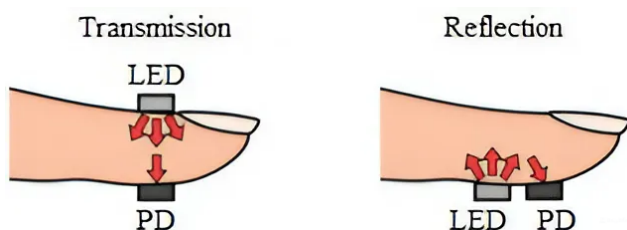


Figure 3. Types of PPG acquisition. Source: Tamura *et al.* [2014] apud Bestbier [2016]

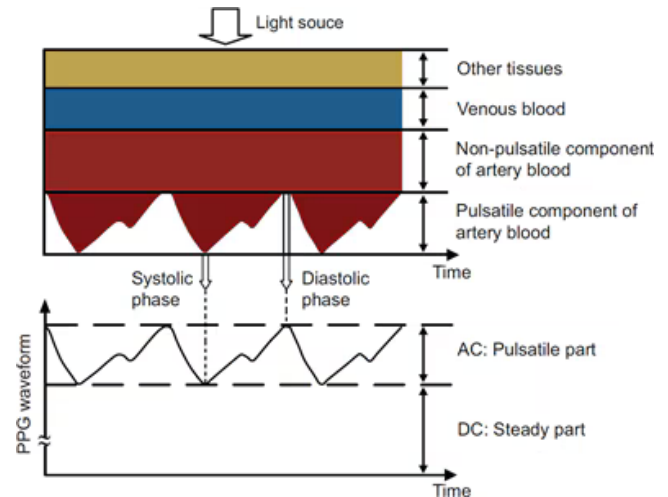


Figure 4. DC and AC components of the PPG signal. Source: Tamura *et al.* [2014]

2.3 Convolutional Neural Network

Convolutional Neural Network (CNN) is a type of deep learning neural network constructed with multiple interconnected layers. This type of neural network specializes in processing grid-structured data, such as images, which are data structured in the form of a pixel matrix. In this type of network, there are a series of mathematical operations aimed at extracting the main characteristics of the data and reducing their dimensionality [Goodfellow *et al.*, 2016].

It is constructed through the sequential coupling of one or several blocks. Each block consists of two layers: the convolution layer and the *pooling* layer. Figure 5 illustrates the general architecture of a CNN.

2.3.1 Convolution Layers

Through their convolution with a two-dimensional matrix, called a filter or *kernel*, CNNs can automatically detect the characteristics of an image. In other words, the *kernel* functions as a feature extractor of the image. In convolution, the *kernel* slides over the pixels of the input image, and the convolution operation is performed [Tervaert *et al.*, 2010].

2.3.2 Pooling Layers

The *pooling* layer aims to statistically represent the previous convolution layer, further reducing the image dimension. In the *pooling* layer, a reduction of values from an image region is performed through a mathematical operation, which can be the average of values, maximum, or minimum [Tervaert *et al.*, 2010].

2.3.3 U-net

Ronneberger *et al.* [2015] states that U-Net is a network composed exclusively of convolutional layers, designed to perform semantic segmentation tasks. The network architecture is formed by a symmetrical pair of networks: the Encoder Network and the Decoder Network. The Encoder Network extracts spatial characteristics from the input signal, while the Decoder Network uses these characteristics to generate a segmentation map. One of the innovative ideas behind U-Net is the use of skip connections, which allow preservation of spatial feature maps, preventing loss during *pooling* operations.

The U-Net architecture has been modified in various

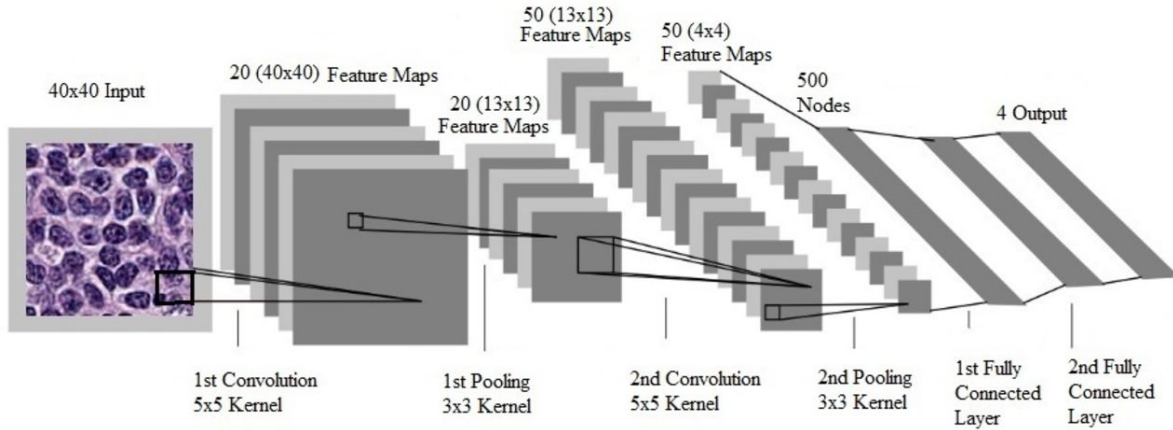


Figure 5. Typical CNN Architecture. Source: Achi *et al.* [2019]

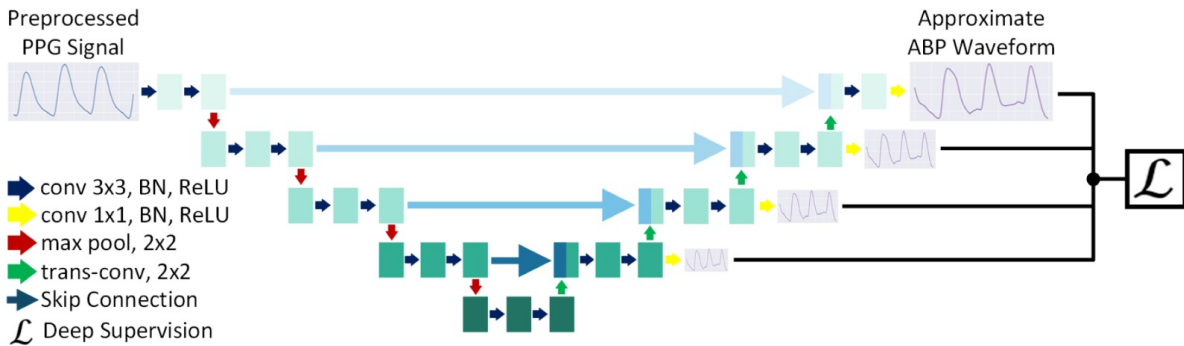


Figure 6. Deeply supervised U-net 1D network. Source: Ibtehaz and Rahman [2020b]

ways to solve different types of problems. In Mahmud *et al.* [2022], a shallower version of U-Net was used for feature extraction from the PPG signal, with the addition of a densely connected Multi-Layer Perceptron (MLP), a type of artificial neural network architecture, to extract the features learned by the network. The results showed that the features extracted by the shallower version of U-Net outperformed most blood pressure prediction techniques found in the literature to date. Therefore, this approach using the adapted U-Net represents a significant contribution to blood pressure prediction based on the PPG signal.

According to Ibtehaz *et al.* [2022], the U-net can be employed to reconstruct one-dimensional (1D) signals, which is primarily a one-to-one regression task. This is achieved by replacing the two-dimensional operations of convolution, pooling, and upsampling with their one-dimensional counterparts. Further states that to obtain a regression output, the final convolutional layer of the network utilizes a linear activation function. Additionally, the concept of deep supervision is also employed in the U-Net. This is a proven technique for reducing overall errors by guiding the learning process of the hidden layers.

In the 1D U-Net or deeply supervised U-Net 1D, an intermediate output is generated, which is a subsampled version of the actual output signal, before each upsampling operation in the decoder [Ibtehaz *et al.*, 2022]. The purpose of this upsampling is to reconstruct the signal with greater precision and detail, capturing important information at different frequency scales. During training, losses are calculated with gradually decreasing weights as one progresses through the

deeper layers of the model, allowing the network to focus on preserving relevant details as the resolution is increased. The diagram of the 1D U-net network is presented in Figure 6.

2.3.4 MultiResU-net

The MultiResUNet 1D model, or MultiResUNet 1D, is an enhanced version of the U-Net model that incorporates MultiRes Blocks (Figure 7b) and ResPath (Figure 7c). The MultiRes blocks employ factorized convolutions for multi-resolution analysis, while the ResPath adds convolutional operations to the shortcut connections to reduce the disparity between the encoder and decoder feature maps. The network utilizes one-dimensional operations for convolution, pooling, and upsampling, with ReLU activation in all layers except the final layer, which uses linear activation. The layers undergo batch normalization but are not supervised in depth [Ibtehaz and Rahman, 2020a].

2.4 MIMIC III

Artificial neural networks depend on specific datasets for training and testing. The Multi-parameter Intelligent Monitoring in Intensive Care (MIMIC III) dataset provided by Physionet is a collection of information obtained from patients in intensive care units (ICU), encompassing a variety of clinical data and monitoring forms. This database contains medical records of approximately 26,000 patients and is carefully anonymized, ensuring the privacy and security of individuals' information [Goldberger *et al.*, 2000]. The MIMIC III offers a wealth of clinical information that is fundamental for the training and testing of neural networks in the context of blood pressure estimation. The available data in-

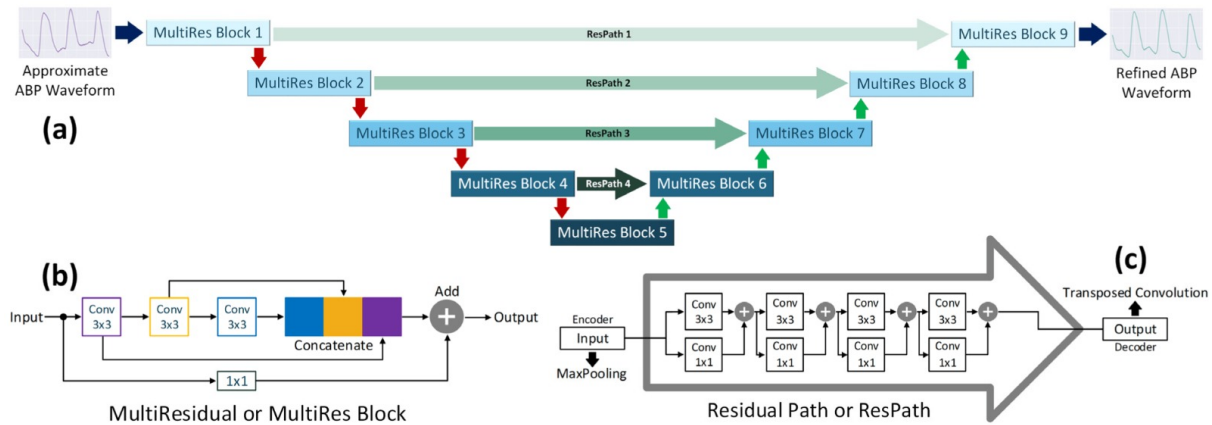


Figure 7. (a) MultiResUNet 1D network, (b) MultiRes Blocks, (c) Res Paths. Source: Ibtehz and Rahman [2020b]

clude vital signs, medical history, laboratory measurements, and other relevant data [Goldberger *et al.*, 2000]. This diversity of clinical information contributes to the robustness and effectiveness of the systems, allowing for a comprehensive and accurate analysis of the obtained results.

3 Related Works

Several studies are dedicated to the development of systemic blood pressure monitoring based on PPG, addressing everything from the conception of what Blood Pressure is, the history of BP measurement devices, conceptualizing PPG, and presenting tests and analyses of neural network applications with the ultimate goal of estimating BP through PPG. Castaneda *et al.* [2018] in their article briefly consider some of the current developments and challenges of wearable PPG based monitoring technologies and then discuss some potential applications of this technology in clinical settings.

Kurylyak *et al.* [2013] present a neural network-based approach for continuous and non-invasive blood pressure estimation using only PPG signals. The authors extracted 21 parameters from each PPG pulse, including systolic upstroke time, diastolic time, and pulse width measurements at various amplitude percentages. Using more than 15,000 heartbeats from the MIMIC-III database for training, they developed a multilayer feed-forward neural network with two hidden layers. Their results demonstrated mean absolute errors of 3.80 ± 3.46 mmHg for systolic and 2.21 ± 2.09 mmHg for diastolic pressure estimation, outperforming linear regression methods and satisfying medical instrumentation standards. The work highlights the potential for implementing blood pressure monitoring on mobile devices.

Leal [2019] presents in his work a device for measuring blood pressure, intended for any person who wants to measure it without leaving home. In his implementation, he used a MAX-30101 sensor, which is an integrated module with pulse oximetry and heart rate monitoring capabilities that uses a non-invasive technique to generate the PPG signal. Regarding the *hardware* of the prototype, an Arduino UNO was used, as the developed platform is based on this development board, which facilitated the reception of the signal from the MAX-30101 sensor.

Moreira [2018] in her study addresses the development of an artificial neural network with the purpose of continu-

ously estimating blood pressure values. The types of methods currently used for blood pressure measurement in clinics, hospitals, and homes are discussed. Her work proposes the use of PPG signals to estimate blood pressure using an artificial neural network that uses as training data the Fast Fourier Transform [Gonzalez and Woods, 2017] applied to the PPG signal obtained from the MIMIC-III database along with blood pressure data. Finally, she concludes that it is possible to measure a person's blood pressure values using PPG and an artificial neural network.

Xing and Sun [2016] introduce and validate a paradigm for beat-to-beat blood pressure estimation using only the PPG signal from fingertips. Their scheme determines the subject-specific contribution to the PPG signal and reduces unwanted interference through appropriate normalization. Features, such as amplitudes and phases of cardiac components, were extracted through a Fast Fourier Transform and were used to train an artificial neural network, which was then used to estimate BP from PPG.

The works listed previously served as the foundation for the development of the current system to estimate blood pressure with PPG. However, the system proposed here differs from previous ones in that it uses not only the MIMIC III database to train the neural network. Rather, it employs computer vision and image processing to extract the PPG signal through videos of the index finger, consequently obtaining heart rate and using it as input for the CNN trained with MIMIC III database. Both Xing and Sun [2016] and Leal [2019] used the MIMIC II database for training and tested the model with new data collected through a dedicated PPG module. Meanwhile, Moreira [2018] focuses on the study and implementation of the neural network to estimate BP, and therefore used the MIMIC III dataset for both training and testing. On the other hand, the current work used an already trained neural network from Ibtehz and Rahman [2020b] with the MIMIC III dataset to estimate BP with data collected from a common smartphone flashlight and its main camera.

4 Methods

The development of the system for estimating blood pressure, as a substitute for conventional methods, can be divided into three main stages: acquisition and processing of the input image through the PPG method, integration of the PPG sig-

nal with a neural network, and finally, statistical analysis of the blood pressure results estimated by the neural network, comparing them with those obtained by a digital device.

4.1 Development Environment

We opted to use a cloud computing service due to the processing demands required by the neural network and the integration with the finger video plethysmography system.

Thus, the choice of Google Colab¹ as a development environment was strategic, as it provided us with the necessary resources for executing the neural network and integration with the plethysmographic signal in the development of the system. The processing capacity and resources offered by the development environment were fundamental for the development of the application.

4.2 Acquisition and Processing of the System Input Image

Initially, two techniques were considered to obtain the PPG signal. The first technique was Eulerian Video Magnification (EVM), proposed by the MIT research group [Wu *et al.*, 2012]. This methodology can enhance low-frequency fluctuations embedded in a visual recording. It is employed to accentuate variations in chromatic intensity associated with the PPG signal, which are commonly low in amplitude and challenging for detection by direct observation without technological assistance.

Thus, by applying EVM to a video capturing blood flow through the skin, it is possible to amplify subtle color variations associated with the PPG signal. However, this approach, in the present study, did not allow for satisfactory results regarding the extraction of the PPG signal. Videos of a person's pulse were recorded for about 10 seconds, and through these, attempts were made to obtain the PPG signal using the video magnification technique. Several image processing techniques were utilized, such as segmentation and the use of Regions of Interest (ROI), which were employed to isolate the region of the person's wrist. However, in both approaches, the generated PPG signals presented a significant amount of noise and oscillations, making them unsatisfactory for analysis.

A second strategy, based on PPG theory, was implemented. The camera of a mobile device with activated illumination was used, with the index finger positioned over both, in order to record changes in the brightness intensity of the green tone present in the subject's finger. The video in this new approach was recorded for about 8 to 9 seconds, to meet the sampling rate requirements of the neural network used. It is also worth noting that the Xiaomi Mi A1 device was the instrument employed in the experiments and presented excellent performance for the PPG application. This device is capable of recording videos with a frame rate of up to 30 frames per second (fps) with a resolution of 1280 × 720 pixels. The selection of the mobile device can impact the results due to the specific characteristics of the camera and illumination.

In the case of the Xiaomi Mi A1, the horizontally parallel arrangement of the camera and flash can facilitate the proper positioning of the finger for filming. This adequate

alignment can contribute to better capturing the variation in brightness intensity of the green color in the finger, which is essential for the precise extraction of the PPG signal.

This information is relevant for purposes of replication and comparison of results, as it demonstrates that the performance of the PPG technique may vary among different cell phone models. Therefore, when conducting similar experiments, it is important to consider the characteristics of the device used, including the arrangement of the camera and flash, to obtain reliable and consistent results.

The PPG technique takes advantage of the fact that blood absorbs different amounts of light at different wavelengths. In the case of the green channel, oxyhemoglobin and deoxyhemoglobin have high absorption to visible light, primarily to the electromagnetic spectrum of the green color [Martins, 2010]. Thus, the absorption of light by human skin is directly proportional to the blood flow in the same location.

As previously mentioned, the quality and precision of the results may vary depending on the proper positioning of the finger in front of the camera and the illumination condition of the flash. Additionally, appropriate image processing and filtering may be necessary to accurately extract the PPG signal from the captured video.

After recording the video of the finger under illumination, the subsequent step involved processing the video using the OpenCV library. The video was read frame by frame, and for each frame, the average intensity of the green channel across all pixels was computed. This spatial averaging process condenses the green channel information of each frame into a single representative value, reducing noise and local variations.

Although the camera captures all three RGB channels, only the green channel is extracted and utilized in our signal processing pipeline, as it provides the clearest photoplethysmographic signal for our application. The red and blue channels are not used in the calculations. This approach of extracting the mean green intensity from each frame, rather than using individual pixel values, helps to obtain a more robust and reliable PPG signal by minimizing the impact of motion artifacts and local illumination variations.

In order to attenuate irregularities and noise present in the green channel signal, a Butterworth band-pass filter was applied. This type of filter is designed to allow the passage of frequencies within a specific range (band), while attenuating frequencies outside this range. The filter formula is presented below, and describes the response of the Butterworth filter.

$$H(s) = \frac{1}{1 + \left(\frac{s}{\omega_0}\right)^{2n}} \quad (3)$$

In this formula, s represents the complex frequency, ω_0 is the central frequency of the passband, and n is the order of the filter.

During the filter development stage, empirical tests were conducted to determine the optimal order. As the filter order increases, its capacity to precisely attenuate frequencies outside the band of interest also increases, making it more selective. However, it is important to consider that an increase in order implies a greater number of coefficients to

¹<https://colab.research.google.com>

be calculated and more operations required to filter the signal.

Higher-order filters require additional computational resources, such as increased processing time and greater memory capacity. In this context, a fifth-order filter was selected after empirical testing with 3 of the 9 participants in our study, as it achieved satisfactory results in the project development. These initial participants provided the baseline data needed to optimize our signal processing parameters before expanding to the full sample. Besides effectively performing the signal filtering role, this filter also allows for conservation of processing resources.

It is also worth highlighting that bidirectional filtering was applied in this filter. This means that the signal is filtered twice: once in the forward direction and once in the reverse direction. This approach results in a linear phase response, preserving the temporal characteristics of the original signal.

This technique is especially useful in applications where the preservation of temporal characteristics is important, such as in biomedical signal processing, where it is necessary to analyze the waveform of the signal over time.

After applying the Butterworth bandpass filter, the filtered green channel signal undergoes an additional smoothing step. A moving average filter with a window size of 5, also empirically tested with the same initial 3 participants, is used to further reduce noise and irregularities present in the signal. This smoothing stage contributes to making the signal more uniform and eliminating unwanted fluctuations.

Subsequently, the smoothed signal is normalized between 0 and 1 using linear min-max normalization. This technique transforms the smoothed signal so that all values fall within the $[0,1]$ range while preserving the relative proportions between the original data points. This normalization process is crucial for adjusting the amplitude of the signal acquired by the camera, bringing it closer to the signals from the MIMIC-III database, which were used for training the neural network. By applying min-max normalization, we ensure that the value range aligns with the signals expected by the neural network, facilitating comparison and interpretation of results. Furthermore, this standardization also preserves the relative variations of the signal, such as the proportional differences between amplitudes.

Afterwards, the signal is resized to meet the input specifications of the neural network. Linear interpolation method is used to adjust the signal length to the desired size of 1024 samples, filling in the intermediate points and ensuring a consistent number of data points.

Finally, the filtered and resulting PPG signal is displayed in a graph. This allows for a visual analysis of the signal and the identification of its main characteristics, such as trends, peaks, and variations over time. Graphical visualization is an important step for understanding and interpreting the filtered PPG signal.

This process of PPG signal acquisition and its processing is illustrated in Figure 8a.

4.3 Neural Network

The neural network used, developed by Ibtehaz and Rahman [2020b], plays a fundamental role in the proposed blood pressure estimation system. The adopted model consists of

two deep convolutional neural networks. The first network, called U-Net 1D, has the function of converting the input signal of the cardiac pulse obtained by PPG into an approximate estimate of blood pressure. Then, the output of this network is used as input for the refinement model, called MultiResU-net 1D, which aims to produce a more accurate waveform closer to the actual blood pressure value.

It is important to mention that the neural network used is publicly available in this place², where it is possible to obtain more detailed information about its operation. Given that this network had already been developed and is publicly available, it was selected for integration into our system. This existing neural network was trained using a robust computational infrastructure consisting of an Intel Core i7-7700 processor (3.6 GHz, 8 MB cache), 16 GB of RAM, and an NVIDIA TITAN XP GPU (12 GB, 1582 MHz), requiring several days of training.

Thus, due to the availability of this already specialized neural network, which is licensed under MIT license and has been thoroughly trained and validated, it was decided to incorporate it into the project as an integral part of the blood pressure estimation system.

The process of developing the neural network model for blood pressure estimation, as described by Ibtehaz and Rahman [2020b], utilized clinical data from the MIMIC-III dataset, processed and organized to optimize neural network training. This dataset contains simultaneous PPG, ECG, and ABP signals, captured in a clinical environment with a sampling rate of 125 Hz. To ensure the quality of the data used, the authors Kachuee et al., apud Ibtehaz and Rahman [2020b], preprocessed the signals, removing episodes with extreme blood pressure values and focusing on signals with specific ranges of DBP and SBP, considered more representative for training.

They segmented the data into episodes of 8.192 seconds (equivalent to 1024 samples), which allowed for precise analysis of each signal without generating excessive computational complexity. To prevent information overlap between training and testing sets, the dataset was carefully divided, ensuring there was no leakage between them. Additionally, signals of varying qualities were included in the training, allowing the neural network to learn to estimate blood pressure from a wide variety of signal conditions, including signals of suboptimal quality.

The segmentation strategy and the inclusion of varied signals helped the neural network become more robust, capable of performing accurate blood pressure estimations in real conditions, demonstrating the effectiveness of the model trained with data derived from Kachuee et al., apud Ibtehaz and Rahman [2020b].

This database was also important in the present work, as through a detailed analysis of the signals present in MIMIC III, it was possible to adapt and adjust the PPG signal obtained from the finger video, adequately integrating it with the neural network.

²<https://github.com/nibtehaz/PPG2ABP>

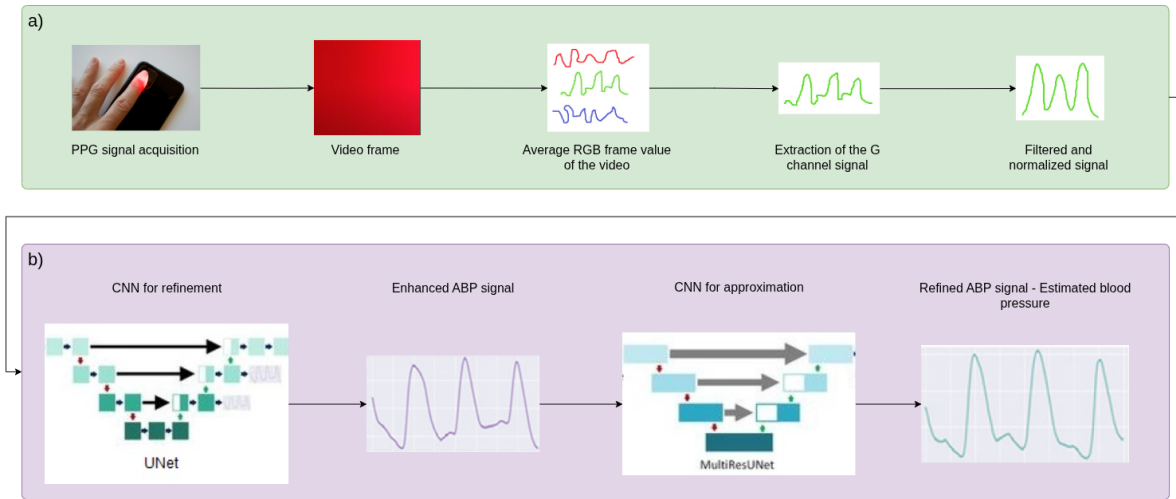


Figure 8. System Diagram: (a) Acquisition and processing of the PPG signal, (b) Integration of the PPG signal with the neural network.

4.4 Integration of the PPG signal with the neural network

After training the neural network, Ibteahz and Rahman [2020b] provides the best trained weights of the specific model for processing PPG signals and generating predictions of the Arterial Blood Pressure (ABP) waveform. These weights represent the parameters learned during training, adjusted to maximize the model's performance in the desired task.

A function was then implemented that integrates the neural network models with the PPG signal to generate a prediction of the ABP waveform, as shown in the flowchart in Figure 9. At the beginning of the function, two specific neural network models are imported to process PPG signals and generate ABP waveform predictions: UNetDS64 and MultiResUNet1D. Next, the function creates instances of these models that are used to make predictions. It is important to note that, at this point, the model instances are initialized without weights.

The pre-trained weights of the models are loaded from the *ApproximateNetwork.h5* and *RefinementNetwork.h5* files. These weights represent the parameters learned during model training and are fundamental for enabling accurate predictions.

Before making predictions, the input PPG signal is resized to fit the form expected by the neural network models. This is necessary because the models expect a batch of samples as input, even if it is only one sample.

The function then predicts the approximate ABP waveform using the first model, UNetDS64. After obtaining the approximate prediction of the ABP waveform, this prediction is passed as input to the second model, MultiResUNet1D, for the final prediction of the refined ABP waveform.

Finally, the predicted ABP waveform is scaled to the correct range using a linear scale. The expected maximum and minimum values are defined as references to obtain the correctly scaled ABP waveform.

Figure 8b provides a visual representation of the steps for integrating the PPG signal with the neural network, offering a clearer view of the process.

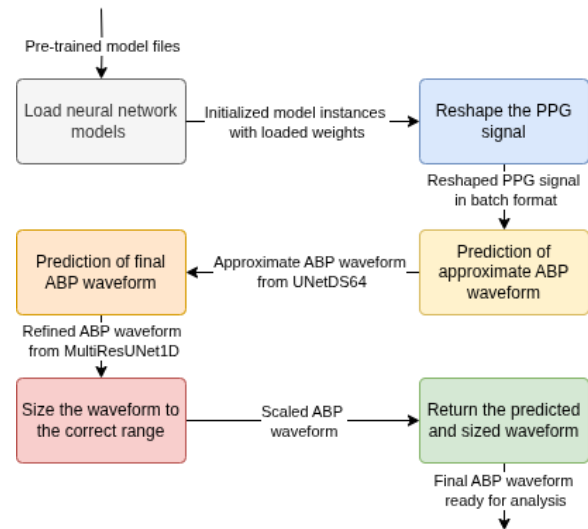


Figure 9. Flowchart of the ABP wave prediction function.

4.5 PPG Signal Preprocessing and BP Extraction

As previously described, the system receives an input PPG signal that has been properly adjusted according to the neural network requirements. This signal undergoes a normalization process and is divided into 1024 samples, as illustrated in Figure 10. This division into fixed-size samples represents the discretization of the PPG signal, facilitating subsequent processing by the neural network.

The videos used to obtain the PPG signal have a duration of approximately 8 to 9 seconds. This duration was chosen considering the 125 Hz sampling rate required by the neural network. This video duration allows for obtaining the necessary 1024 samples, ensuring that each sample represents a measurement of the PPG signal at a specific moment in time.

Using the PPG signal example in the ABP wave prediction algorithm, it is possible to obtain the blood pressure estimate, resulting in the signal illustrated in Figure 11. From this signal, it is possible to extract important information about blood pressure, such as the systolic and diastolic pressure values. The maximum peak value in the signal corresponds to the systolic pressure, while the minimum value of

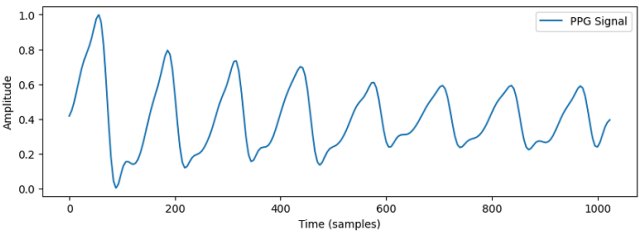


Figure 10. Normalized PPG signal.

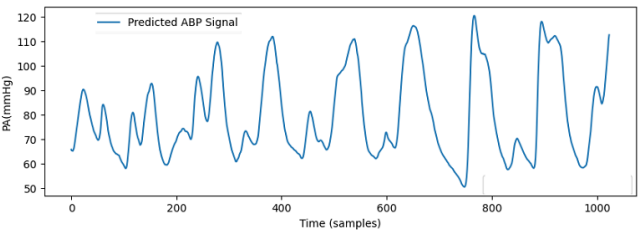


Figure 11. Estimated blood pressure signal.

the valleys represents the diastolic pressure.

To improve the accuracy of the estimated diastolic pressure calculation, approximately 10 system tests were conducted. During these tests, it was observed that the diastole estimation showed a more pronounced error due to a sharp descent in one of the valleys of the estimated wave. This atypical oscillation compromised the precise correspondence between the estimated value and the actual diastolic pressure value. This occurrence was present in all ABP waves in the output of the refinement neural network, similar to Figure 11.

5 Results

Based on these results, it was necessary to find a solution that would circumvent this discrepancy and make the estimation more reliable without compromising the integrity of the estimated signal. After careful analysis and some empirical tests, it was found that an increase of approximately 17% in the value of the lowest valley of the estimated wave would be able to compensate for this oscillation and reduce the pronounced error in the diastolic pressure estimation. This improved the accuracy of the system as a whole.

Thus, we can observe the result generated by the system in Table 1. It presents the values estimated by the system and the actual values that were obtained using the Omron HEM-6124 digital device (Figure 12). The absolute error calculation is also shown.

Table 1. Output system result.

Item	Value
Peak value (estimated systolic pressure)	123.14 mmHg
Valley value (estimated diastolic pressure)	61.23 mmHg
Actual systolic pressure	128 mmHg
Actual diastolic pressure	69 mmHg
Absolute error in systolic pressure	5.14 mmHg
Absolute error in diastolic pressure	7.77 mmHg

To enhance the system’s accuracy and evaluate its reliability in blood pressure estimation, an analysis was conducted on a sample of nine individuals. Additional videos were recorded; however, the recording exceeded the 8 seconds prescribed by the network, therefore only 9 samples

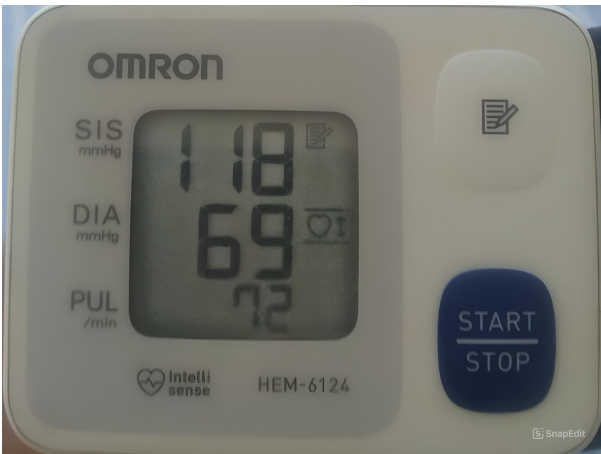


Figure 12. Digital device result.

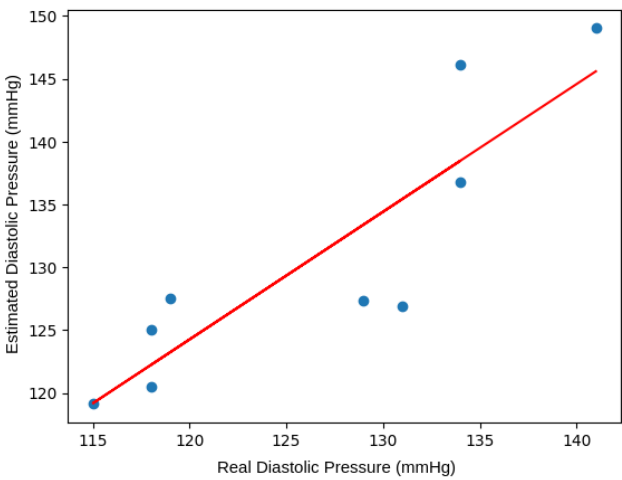


Figure 13. Scatter plot of Real vs. Estimated Systolic Pressure.

were used. During this analysis, we estimated these individuals’ blood pressure values using the system in question and compared them with readings obtained from a digital blood pressure device, measured immediately after video recording, both on the left arm.

The statistical analysis of the collected data provided significant information about how close the estimated values are to the actual values measured by the digital device. These statistical data provided a comprehensive view of the system’s performance, identifying possible deviations or discrepancies in the estimates.

Figure 13 presents the scatter plot graph for systolic pressure. It is observed that the values estimated by the system demonstrated close agreement with the actual values obtained from the digital measurement device. The points follow a linear trend, indicating a positive correlation between estimates and actual values. This result reinforces the system’s reliability in estimating systolic pressure.

In Figure 14, it can be noted that some points are more distant from the linear trend and show greater dispersion. This can be attributed to the fact that some estimates showed more significant errors compared to the actual measured values. This greater variability in results suggests that the system may have more difficulty accurately estimating diastolic pressure compared to systolic pressure.

Based on this sample, it was possible to calculate the

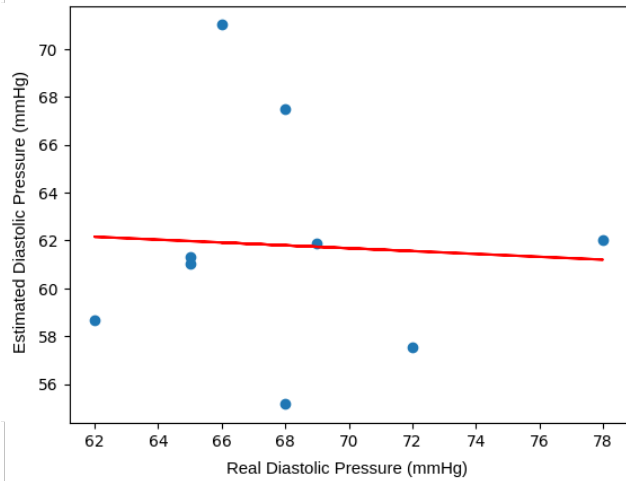


Figure 14. Scatter plot of Real vs. Estimated Diastolic Pressure.

Mean Absolute Error (MAE) of blood pressure estimates, along with its uncertainty represented by the standard deviation. For systolic pressure, the MAE was 5.65 mmHg, with a possible variation of up to ± 3.27 mmHg relative to actual values. For diastolic pressure, the MAE was determined to be 7.51 mmHg with an uncertainty of ± 4.65 mmHg. These error values follow and confirm the system's tendency, also represented in the linear regression graph presented previously.

In Table 2, we present a comparison between the present work and other similar studies, highlighting the MAE values. It is important to note that previously related works, such as Moreira [2018] and Leal [2019], although fundamental for the theoretical foundation, did not provide MAE metrics, making it impossible to include their data in this table.

Thus, we used the base neural network work used in the project by Ibtezhaz and Rahman [2020b], named PPG2ABP in the table. Additionally, it is also possible to compare with the work of dos Santos Cardoso *et al.* [2021], which conducts a comparative study between the LSTM (*Long Short-Term Memory*) neural network, used in their work, and the MLP (*Multi Layer Perceptron*) network. This study shows that using temporal characteristics of the PPG signal as input parameters can result in better outcomes. In the table, this work is identified as LSTM for easier identification.

In addition to these two, we can make a comparison with the work of Kurylyak *et al.* [2013], named after the first author, Yuriy Kurylyak. This work uses Artificial Neural Networks (ANNs) to estimate blood pressure through PPG signals from a database.

Table 2. Mean Absolute Error Comparison.

Paper	SBP (mmHg)	DBP (mmHg)
PPG2ABP	5.727 ± 9.162	3.449 ± 6.147
Yuriy Kurylyak	3.80 ± 3.46	2.21 ± 2.09
LSMT	7.53 ± 7.34	12.57 ± 10.33
Ours	5.65 ± 3.27	7.51 ± 4.65

Thus, we can infer that the present study excels in SBP estimation, demonstrating a lower error rate, second only to the work of Yuriy Kurylyak. Regarding DBP, although it shows a higher error when compared to the PPG2ABP and Yuriy Kurylyak studies, the present work demonstrates supe-

rior performance when compared to the LSTM study.

It is important to note that the related works mentioned in Table 2 utilize different validation approaches for their neural networks. For instance, the PPG2ABP study Ibtezhaz and Rahman [2020b] employed a 10-fold cross-validation methodology, where 90% of the training data was used to train the model, and the remaining 10% for validation. Similarly, Kurylyak *et al.* [2013] used the MIMIC database with specific validation protocols, while the LSTM study dos Santos Cardoso *et al.* [2021] implemented its own validation strategy. Although the input PPG signals originate from different sources compared to the present work, both the current study and similar works utilize actual PPG signals and estimate the arterial pressure wave through neural networks. Therefore, the comparison of mean absolute error between them provides a valid performance benchmark.

6 Conclusion

In the present work, an alternative method was developed to estimate blood pressure, aiming to offer a non-intrusive approach with the potential to facilitate population access to this vital information. Knowing that there is a growing incidence of cardiac problems worldwide, it is possible to understand the importance of seeking solutions that are more accessible and convenient for cardiovascular health monitoring. In this sense, this project stands out for offering a promising alternative that can contribute to early detection and more effective monitoring of these problems.

As seen in the previous statistical analyses, this project presents considerable performance for SBP estimation when compared with similar works, which is a very positive point in its development and reliability. However, this same project presents a slightly higher error in predicting DBP values, indicating that it can be improved to be considered more accurate and reliable in its estimation.

Several factors can influence the more pronounced error in DBP prediction. One of these factors may be the presence of persistent noise during the diastolic phase of PPG signal acquisition. In the present work, the use of a PPG signal obtained from a video of the illuminated finger introduces certain complexities in signal processing, which can still be improved to reduce error values in the estimation of both DBP and SBP.

PPG2ABP served as the basis for this study, as we used the neural network developed in it. However, it is worth remembering that the PPG signals used in PPG2ABP originated from the MIMIC III database, which extracts these signals from monitoring hospitalized patients, where plethysmographic sensors are commonly used. This differentiation in signal acquisition may contribute to obtaining more accurate results in PPG2ABP.

We therefore seek to improve the performance of DBP estimation, approaching the results obtained in the PPG2ABP work, which obtained more favorable results in this metric. It is believed that with improvements in PPG signal processing and refinements in its acquisition, it will be possible to reduce the error in DBP estimation and, consequently, achieve values closer to those obtained in the base work.

One of the techniques that can be used is Wiener deconvolution, used to deconvolve or defocus a distorted signal. It is especially useful when the original signal is corrupted by a known additive noise. Wiener deconvolution attempts to recover the original signal by estimating the filter that caused the distortion and applying an inversion or appropriate compensation.

In the context of the present work, it can be useful because it is a tool with the potential to remove or mitigate unwanted noise in close-up video recordings. The main idea is to model noise distortion as a stochastic process and then apply the Wiener deconvolution technique to estimate the original signal.

Another factor that can increase the accuracy of the system and reduce error values is the use of a larger sample in the system. In general, increasing the sample size tends to improve the accuracy of estimates and reduce error. This is because a larger sample allows for a more comprehensive and accurate representation of the phenomenon under study. Thus, there is an intention to test the system with more samples, so that it is possible to capture greater variation and reduce the impact of random fluctuations on the results.

In the context of blood pressure estimation, a larger sample can provide a more complete view of the characteristics and patterns of the PPG signal, allowing a better adjustment of the model used in the estimation. Additionally, a larger sample size also allows for more robust validation of the method, since the results are based on a larger number of observations.

Despite this higher error in DBP estimation, the system still has another positive point, as in addition to generating SBP and DBP estimates, it can estimate the ABP waveform itself, which can be used to robustly estimate cardiovascular anomalies from waveform patterns and BP parameters. ABP waveforms are generally collected invasively, and with the system, they can be reliably estimated from externally acquired PPG signals.

The proposed improvements for the system aim primarily to enhance DBP estimation. Additionally, we seek to offer users a more pleasant experience through the creation of an intuitive and user-friendly graphical interface. This interface will facilitate interaction with the system and understanding of the results obtained.

Another improvement that can be implemented is the inclusion of a blood pressure classification system. This feature would allow categorizing the results obtained into blood pressure ranges, such as normal, elevated, or hypertension. This classification would help users better understand their blood pressure levels and, together with medical assistance, take appropriate measures to care for their cardiovascular health.

Furthermore, the expansion of the system to mobile versions is an interesting perspective. This would allow the system to be accessed and used on mobile devices, such as smartphones, providing greater convenience and flexibility to users. The possibility of using cell phone cameras for real-time monitoring is a promising idea, as it could offer a more practical and continuous form of blood pressure measurement.

These future implementations would contribute to mak-

ing the system more complete and comprehensive, offering a more accessible and convenient solution for blood pressure monitoring. It is important to emphasize that, even with the availability of these improvements, it is essential that users seek the guidance of a healthcare professional to obtain a complete and accurate assessment of their cardiovascular condition. Medical assistance is essential for interpreting results, obtaining personalized recommendations, and appropriate monitoring of blood pressure treatment. The combination of system use with medical support will provide a comprehensive and safe approach to cardiovascular health care.

Declarations

Authors' Contributions

GSMA performed the experiments and wrote the manuscript. CEG supervised the research, contributed to manuscript revision, and provided critical review and editing. All authors read and approved the final manuscript.

Competing interests

The authors declare that they have no competing interests.

Availability of data and materials

The datasets and softwares generated during the current study will be made upon request.

References

- Achi, H. E., Belousova, T., Chen, L., Wahed, A., Wang, I., Hu, Z., Kanaan, Z., Rios, A., and Nguyen, A. N. D. (2019). Automated diagnosis of lymphoma with digital pathology images using deep learning. *Annals of Clinical and Laboratory Science*, 49(2):153–160. PMID: 31028058. Available in: <https://pubmed.ncbi.nlm.nih.gov/31028058/>.
- Berne, R. M., Levy, M. N., Koeppen, B. M., and Stanton, B. A. (2008). *Berne & levy physiology*. Elsevier Brasil. ISBN: 978-0323045827.
- Bestbier, A. (2016). *Monitoring core temperature, heart rate, respiratory rate and EEG of an infant through a wireless ear probe*. PhD thesis, Stellenbosch University. DOI: 10.13140/RG.2.2.29709.95203.
- Castaneda, D., Esparza, A., Ghamari, M., Soltanpur, C., and Nazeran, H. (2018). A review on wearable photoplethysmography sensors and their potential future applications in health care. *International journal of biosensors & bioelectronics*, 4(4):195. DOI: 10.15406/ijbsbe.2018.04.00125.
- dos Santos Cardoso, G., Gomes Lucas, M., and dos Santos Cardoso, S. (2021). Predição de pressão sanguínea através de sinais de fotopletiśmografia usando redes neurais MLP e LSTM. *Revista Brasileira de Física Médica*, 15:637. DOI: 10.29384/rbfm.2021.v15.19849001637.
- Galloway, B. (2012). Biomedical Sensors and Instruments, [Book Reviews]. *IEEE Pulse*, 3(3):70–70. DOI: 10.1109/MPUL.2012.2189670.
- Goldberger, A. L., Amaral, L. A., Glass, L., Hausdorff, J. M., Ivanov, P. C., Mark, R. G., Mietus, J. E., Moody, G. B., Peng, C.-K., and Stanley, H. E. (2000). PhysioBank, PhysioToolkit, and PhysioNet: components of a new research

- resource for complex physiologic signals. *Circulation*, 101(23):e215–e220. DOI: 10.1161/01.CIR.101.23.e215.
- Gonzalez, R. and Woods, R. (2017). *Digital Image Processing Global Edition*. Pearson Deutschland, 4th edition. ISBN: 978-1-292-22304-9.
- Goodfellow, I., Bengio, Y., and Courville, A. (2016). *Deep Learning*. MIT Press. Available in: <http://www.deeplearningbook.org>.
- Hsu, Y.-C., Li, Y.-H., Chang, C.-C., and Harfiya, L. N. (2020). Generalized deep neural network model for cuffless blood pressure estimation with photoplethysmogram signal only. *Sensors*, 20(19). DOI: 10.3390/s20195668.
- Ibtehaz, N., Mahmud, S., Chowdhury, M. E., Khandakar, A., Salman Khan, M., Ayari, M. A., Tahir, A. M., and Rahman, M. S. (2022). Ppg2abp: Translating photoplethysmogram (ppg) signals to arterial blood pressure (abp) waveforms. *Bioengineering*, 9(11):692. DOI: 10.3390/bioengineering9110692.
- Ibtehaz, N. and Rahman, M. S. (2020a). MultiResUNet: Rethinking the U-Net architecture for multimodal biomedical image segmentation. *Neural Networks*, 121:74–87. DOI: 10.1016/j.neunet.2019.08.025.
- Ibtehaz, N. and Rahman, M. S. (2020b). Ppg2abp: Translating photoplethysmogram (ppg) signals to arterial blood pressure (abp) waveforms using fully convolutional neural networks. *arXiv preprint arXiv:2005.01669*. DOI: 10.48550/arXiv.2005.01669.
- Introcaso, L. (1998). Aspectos históricos da hipertensão: História da medida da pressão arterial. *HiperAtivo*, 5(2):79–82. Available in: <http://departamentos.cardiol.br/dha/revista/5-2/asphiship.pdf>.
- Junqueira, L. F. (2006). Considerações básicas sobre a organização estrutural e a fisiologia do aparelho cardiovascular. *Laboratório Cardiovascular da Universidade de Brasília*, 10(01). DOI: 10.13140/RG.2.1.1503.7605.
- Kalkhaire, S. D. and Puranik, V. G. (2016). Remote detection of photoplethysmographic signal and SVM based classification. In *2016 IEEE International Conference on Advances in Electronics, Communication and Computer Technology (ICAECCT)*, pages 128–132. DOI: 10.1109/ICAECCT.2016.7942568.
- Kohlmann, N. E. B. and Kohlmann Jr, O. (2011). Histórico e perspectivas da medida da pressão arterial. *Revista Hipertensão*, 14(2):5–13. ISSN: 1809-4260.
- Kurylyak, Y., Lamonaca, F., and Grimaldi, D. (2013). A Neural Network-based method for continuous blood pressure estimation from a PPG signal. In *2013 IEEE International instrumentation and measurement technology conference (I2MTC)*, pages 280–283. IEEE. DOI: 10.1109/I2MTC.2013.6555424.
- Leal, J. F. U. (2019). Desenvolvimento de um Protótipo de Monitoramento de Pressão Arterial Sistêmica Baseado em Fotopletismografia. Dissertação (Mestrado em Engenharia Elétrica), Universidade Federal do Espírito Santo, Vitória. Available in: <http://repositorio.ufes.br/handle/10/13649>.
- Mahmud, S., Ibtehaz, N., Khandakar, A., Tahir, A. M., Rahman, T., Islam, K. R., Hossain, M. S., Rahman, M. S., Musharavati, F., Ayari, M. A., et al. (2022). A shallow U-Net architecture for reliably predicting blood pressure (BP) from photoplethysmogram (PPG) and electrocardiogram (ECG) signals. *Sensors*, 22(3):919. DOI: 10.3390/s22030919.
- Martins, R. M. S. (2010). Desenvolvimento de um sensor de fotopletismografia para monitorização cardíaca para aplicação no pulso. Dissertação (Mestrado) em Engenharia Biomédica, Universidade de Coimbra (Portugal). Available in: <https://hdl.handle.net/10316/14086>.
- Moreira, F. G. (2018). Estudo sobre a estimativa da pressão arterial utilizando dados de fotopletismografia da base MIMIC e uma rede neural artificial. Trabalho de Conclusão de Curso (Graduação), Universidade Tecnológica Federal do Paraná. Available in: <http://repositorio.utfpr.edu.br/jspui/handle/1/14601>.
- Ronneberger, O., Fischer, P., and Brox, T. (2015). U-Net: Convolutional Networks for Biomedical Image Segmentation. In *Medical Image Computing and Computer-Assisted Intervention—MICCAI 2015: 18th International Conference, Munich, Germany, October 5–9, 2015, Proceedings, Part III 18*, pages 234–241. Springer. DOI: 10.1007/978-3-319-24574-4_28.
- Sousa, A. L. L., Jardim, P. C. B. V., Mendonça, B. C., Jardim, T. d. S. V., Barroso, W. K., Rodrigues, R. B., and Carneiro, S. B. (2011). Medida casual da pressão arterial: vantagens e desvantagens no diagnóstico e tratamento da hipertensão arterial. *Revista Hipertensão*, 14(2):45–50. ISSN: 1809-4260.
- Suárez, L. (2003). *Técnico Auxiliar de Geriatria. Manual. Temario. E-book*. MAD-Eduforma. ISBN: 9788466530323.
- Tamura, T., Maeda, Y., Sekine, M., and Yoshida, M. (2014). Wearable Photoplethysmographic Sensors—Past and Present. *Electronics*, 3. DOI: 10.3390/electronics3020282.
- Tervaert, T. W. C., Mooyaart, A. L., Amann, K., Cohen, A. H., Cook, H. T., Drachenberg, C. B., Ferrario, F., Fogo, A. B., Haas, M., de Heer, E., et al. (2010). Pathologic classification of diabetic nephropathy. *Journal of the American Society of Nephrology*, 21(4):556–563. DOI: 10.1681/ASN.2010010010.
- Wu, H.-Y., Rubinstein, M., Shih, E., Guttag, J., Durand, F., and Freeman, W. (2012). Eulerian video magnification for revealing subtle changes in the world. *ACM Trans. Graph.*, 31(4). DOI: 10.1145/2185520.2185561.
- Xing, X. and Sun, M. (2016). Optical blood pressure estimation with photoplethysmography and fft-based neural networks. *Biomedical optics express*, 7(8):3007–3020. DOI: 10.1364/BOE.7.003007.
- Zhou, B., Carrillo-Larco, R. M., Danaei, G., Riley, L. M., Paciorek, C. J., Stevens, G. A., Gregg, E. W., Bennett, J. E., Solomon, B., Singleton, R. K., et al. (2021). Worldwide trends in hypertension prevalence and progress in treatment and control from 1990 to 2019: a pooled analysis of 1201 population-representative studies with 104 million participants. *The Lancet*, 398(10304):957–980. DOI: 10.1016/S0140-6736(21)01330-1.